EG&G

ENERGY MEASUREMENTS GROUP

SRO-304
March 1982

DRAFT

SYSTEMATIC EVALUATION PROGRAM STRUCTURAL REVIEW OF THE OYSTER CREEK NUCLEAR POWER PLANT DRYWELL CONTAINMENT STRUCTURE UNDER COMBINED LOADS

By

A. G. Debeling
C. Y. Liaw

Work Performed for Lawrence Livermore National Laboratory under U.S. Department of Energy Contract No. DE-AC08-76 NVO 1183.

SAN RAMON OPERATIONS
2801 OLD CROW CANYON ROAD
SAN RAMON, CALIFORNIA 94583

DRAFT

FOREWORD

The U.S. Nuclear Regulatory Commission (NRC) is conducting a Systematic Evaluation Program (SEP), which is a plant-by-plant reassessment of the safety of 11 operating nuclear reactors that received construction permits between 1956 and 1967. Because many safety criteria have changed since these plants were licensed, the purpose of the SEP is to develop a current, documented basis for the safety of these older facilities.

Seismic analyses for a Safe Shutdown Earthquake (SSE) for the Oyster Creek Nuclear Power Plant had been performed in a previous study of selected plant structures, systems, and components from generic groups of equipment. The results of these analyses were reported in an earlier SEP report, NUREG/CR-1981. In the study reported on here, the containment structure was selected for further evaluation of the combined effect of the SSE and the design basis accident (DBA), including evaluation of both the loss of coolant accident (LOCA) and the main steam line break (MSLB).

DRAFT

ACKNOWLEDGEMENTS

The authors wish to thank P. Y. Chen and S. Brown, technical monitors of this work at the Office of Nuclear Reactor Regulation (NRR), for their continuing support , and T. A. Nelson and T. Y. Lo of Lawrence Livermore National Laboratory (LLNL), who provided project management support and reviewed the report.

This report is a collective effort by the following people: A. G. Debeling and C. Y. Liaw, of EG&G/San Ramon Operations, who conducted the structural reevaluation of the drywell containment structure, and T. A. Nelson and T. Y. Lo of Lawrence Livermore National Laboratory.

DRAFT

ABSTRACT

A reassessment of the drywell containment structure of the Oyster Creek Nuclear Power Plant was performed for the Nuclear Regulatory Commission as part of the Systematic Evaluation Program. Conclusions about the ability of the drywell containment structure to withstand the combined effect of a Safe Shutdown Earthquake (SSE) and a Design Basis Accident (DBA) which include either a double ended recirculation line break (LOCA) or main steam line break (MSLB), are presented. Both the SSE and DBA loads employed in this reassessment came from previous studies conducted by the U.S. Nuclear Regulatory Commission (NRC).

This reassessment focused mainly on the overall structural integrity of the drywell containment to withstand an SSE plus DBA. The stress intensity limits of Subsection NE of the 1977 ASME Boiler and Pressure Vessel Code, Section III, Division 1 for the Design and Service Conditions were used as the compliance criteria for structural reassessment. Design Condition is described by the combination deadweight, SSE, and pressure loads from a DBA. Service Condition is described by the Design Condition combination plus the thermal loads from the DBA.

DRAFT

CONTENTS

DRAFT

LIST OF ILLUSTRATIONS

LIST OF TABLES

DRAFT

CHAPTER 1
INTRODUCTION

1.1 SCOPE OF WORK

Structural reassessment of nuclear power plants is one facet of the Systematic Evaluation Program (SEP) being conducted by the Nuclear Regulatory Commission (NRC). This report is a structural review of the Oyster Creek drywell containment structure. The overall structural integrity of the drywell was evaluated based on the stress intensity limits for the design and service conditions defined in the ASME Boiler and Pressure Vessel Code, Section III, Subsection NE, 1977. In this reassessment, the design conditions included a Safe Shutdown Earthquake (SSE), as represented by the Reg. Guide 1.60 response spectra, which is scaled to 0.17g peak ground acceleration, and the pressure due to a postulated Design Basis Accident (DBA). The DBA consists of either a loss of coolant accident (LOCA) or a main steam line break (MSLB). Service conditions were defined as the design condition loads plus thermal loads caused by the DBA.

In this analysis, the seismic event and the worst of the main steam line breaks (MSLB) and double ended recirculation line breaks were applied as if they occurred simultaneously. The thermal and pressure loading conditions due to the DBA are based on the analysis discussed in Reference 1. The seismic stress evaluation is an extension of the analysis presented in "Seismic Review of the Oyster Creek Nuclear Power Plant as part of the SEP Program" (Reference 2).

Because the primary objective of this analysis is to determine the drywell's ability to perform containment functions when subjected to the combined action of the DBA, deadweight, and seismic loads, no local loads or flooding conditions were considered. Reinforcement around penetrations in the drywell were assumed to be as strong as the drywell shell;

DRAFT

therefore, the local discontinuity effect of the penetrations on the overall shell stresses was neglected. Hence, an axisymmetric shell model was used in this analysis.

1.2 STRUCTURE DESCRIPTION

The drywell containment structure of the Oyster Creek plant houses the reactor vessel, reactor coolant recirculating loops, and other components associated with the reactor system. The structure is a combination spherical, cylindrical, and 2:1 ellipsoidal dome that resembles an inverted light bulb. The spherical section has an inside diameter of 70 ft which reduces down to 33 ft at the cylindrical portion connecting the sphere to the dome. The structure is approximately 99 ft high. The plate thickness varies from a maximum of 2.56 in. at the transition of the sphere and cylindrical section down to a minimum of 0.640 in. at the cylindrical section. The dome wall thickness is 1.18 in. Figure 1 illustrates the drywell structure along with pertinent dimensions. The top closure, which is 33 ft in diameter, is made with a double tongue and groove seal which permits periodic checks for tightness. Ten vent pipes, 6 ft in diameter, are equally spaced around the circumference to connect the drywell and vent headers in the pressure absorption chamber (Torus).

A 3-inch gap between the drywell and concrete biological shield is filled with foam material that provides insulation but no significant structural support. An upper lateral seismic restraint attached to the cylindrical portion of the drywell at an elevation of 82.17 ft, allows for thermal, deadweight, and pressure deflection, but not for lateral movement due to seismic excitation. All penetration for piping, instrumentation lines, vent ducts, electrical lines, equipment accesses, and personnel entrance have expansion joints and double seals where applicable. A sand entrenchment surrounds the drywell from an elevation of 8.93 ft (foundation-steel interface) to 12.25 ft. The entrenchment acts as a transition buffer for loads generated at the shell-foundation region.

DRAFT

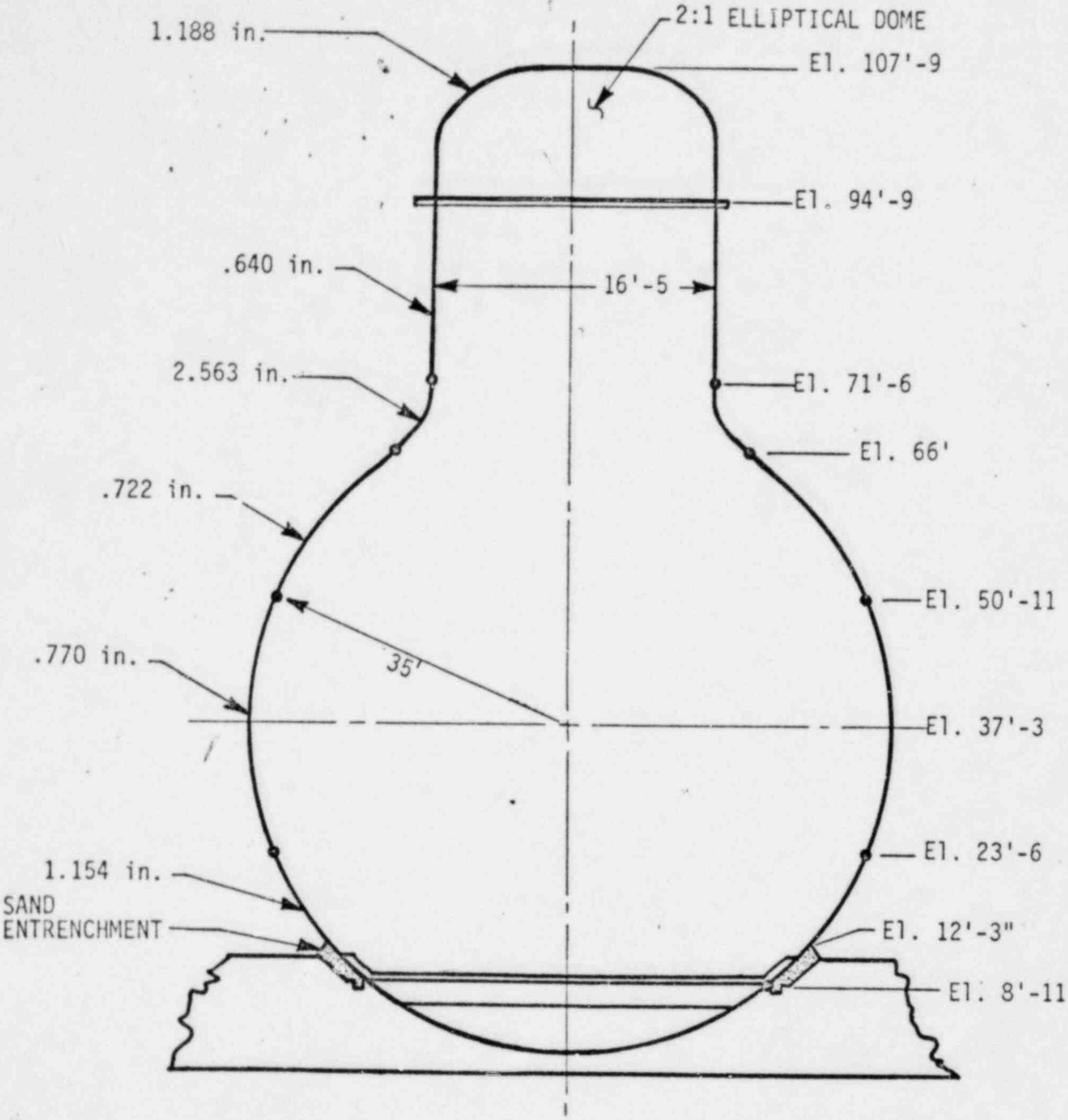

Figure 1. Drywell structure.

DRAFT

1.3 LOADS AND LOAD COMBINATION

The loads that were considered in this analysis are the deadweight loads, the seismic loads, and the pressure and thermal loads due to a postulated Design Basis Accident (DBA). The peak drywell stresses due to these loads were combined algebraically, but with the worst combination of signs possible (which is a conservative approach).

1.3.1 Deadweight Loads

Deadweight loads were generated by multiplying the steel weight density (0.238 lbw/in^3) by the drywell volume. The dimensions used to determine the drywell volume were based on the structural drawings contained in the Oyster Creek FSAR (Reference 6).

1.3.2 Seismic Loads

Figures 2 and 3 illustrate the recommended moment and shear loads that came from the SSE analysis of the drywell, which is contained in Reference 2. A Reg. Guide 1.60 spectra with peak ground acceleration of 0.22 g's was used to generate these values. In the time span between this analysis and the SSE analysis presented in Reference 2, a site-specific spectra with a peak ground acceleration of 0.17 g's was approved by the NRC. The information from the NRC contained in Reference 8 allows two options if reanalysis is needed: (1) to scale down the previous analysis (which used a Reg. Guide 1.60 spectra) by the ratio of the new site-specific peak ground acceleration to that of the peak ground acceleration used in the original analysis, and (2) to use the new site-specific spectra for reanalysis. For this analysis the scaling method using the ratio 0.17/0.22 was used to determine the seismic loads that were applied to the drywell. It should be noted that a Reg. Guide 1.60 spectra with peak ground acceleration of 0.17 g's envelops the new Oyster Creek site-specific spectra; therefore the seismic loads used in this analysis are conservative.

DRAFT

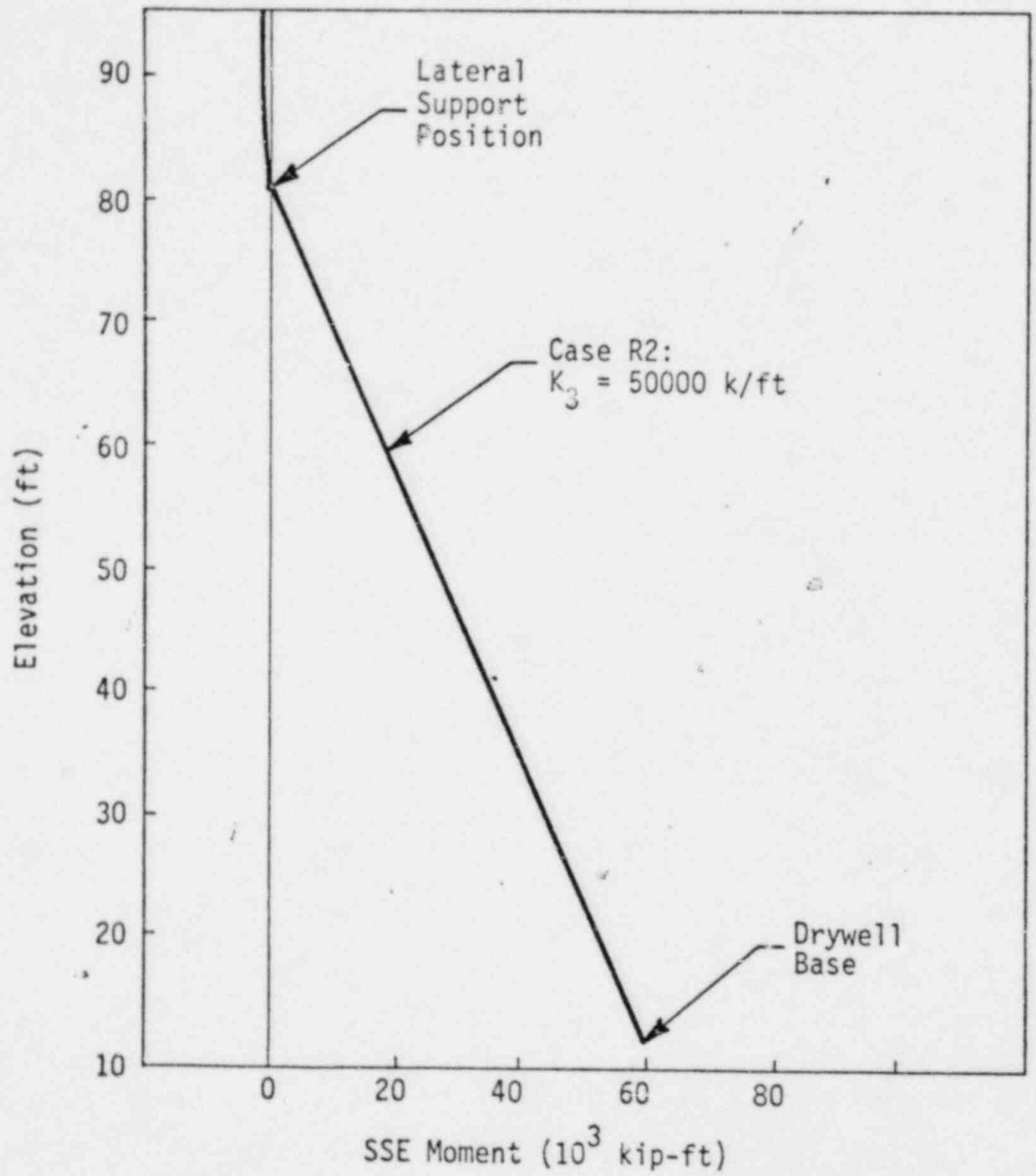

Figure 2. Drywell bending moment due to SSE.

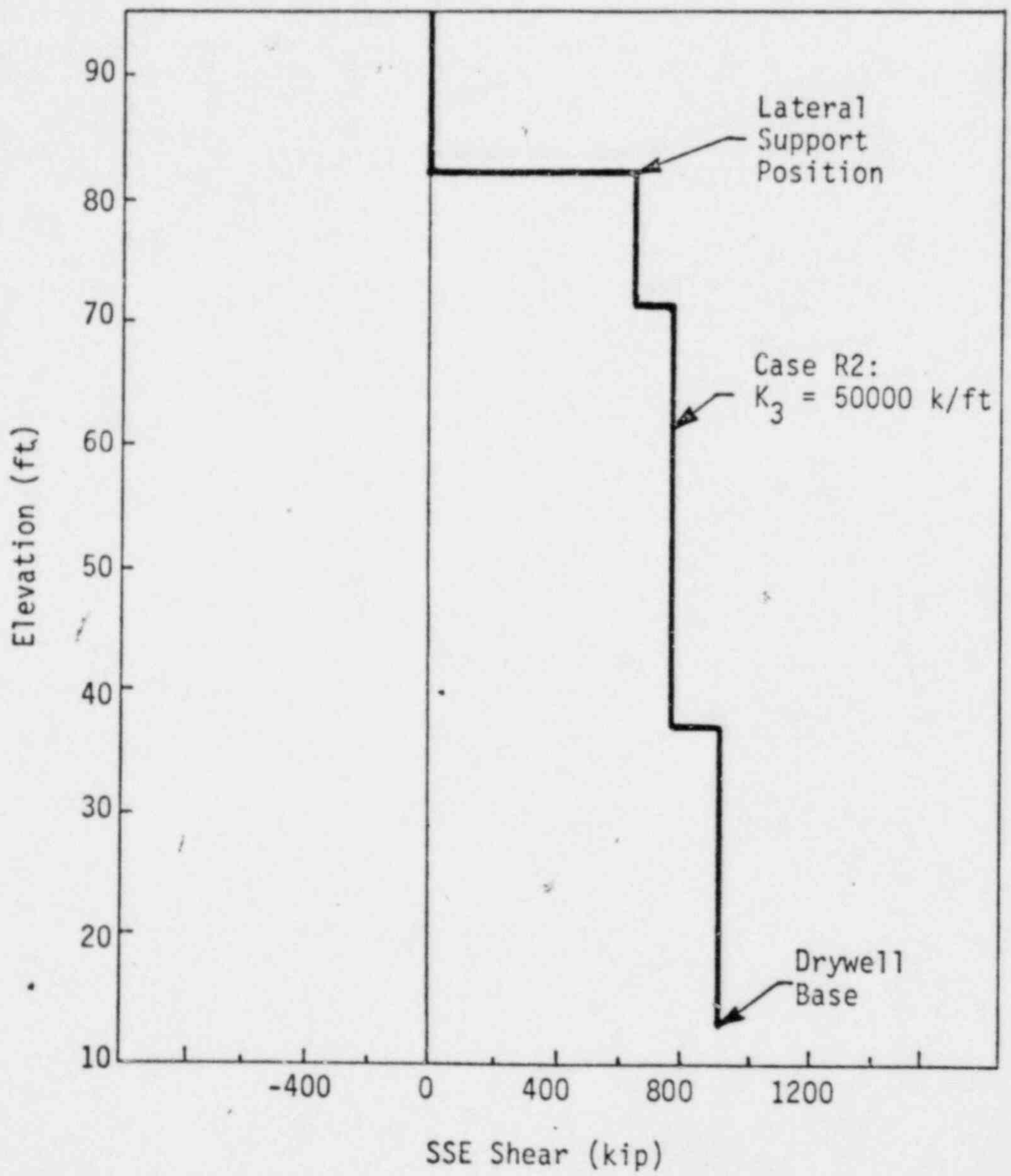

Figure 3. Drywell shear load due to SSE.

DRAFT

1.3.3 Design Basis Accident (DBA) Loads

A spectra of possible recirculation and main steam line breaks were analyzed to determine the peak post-accident pressure and temperature response of the drywell. The maximum calculated peak pressure response was due to a double ended recirculation line break and the temperature response was caused by a 0.75 ft^2 main steam line break. Reference 1 contains detailed information on the mass energy release analysis for these postulated breaks and formed the basis for determining the temperature and pressure loads used in this analysis.

Because the temperature response caused by the 0.75 ft^2 main steam line break was slightly higher than the temperature response due to the double ended recirculation line break, the main steam line break temperature response and the double ended recirculation line break pressure response were combined to form a conservative pseudo-event. Deadweight and seismic loads were also combined with this pseudo-event, which eliminated the need to perform a separate load combination analysis for main steam line and double ended recirculation line break cases.

Pressure Loads

Figures 4 and 5 illustrate the drywell pressure history response predicted for a double ended recirculation line break and a 0.75ft^2 main steam line break, respectively. A maximum pressure of 37 psig at 4.5 seconds, caused by a double ended recirculation line break, was applied to the drywell to determine structural adequacy.

Thermal Loads

Figures 6 and 7 illustrate the drywell atmospheric temperature response generated by the 0.75ft^2 main steam line break and the double ended recirculation line break, respectively. The metal temperatures will actually be less and will lag in time behind the atmospheric temperatures.

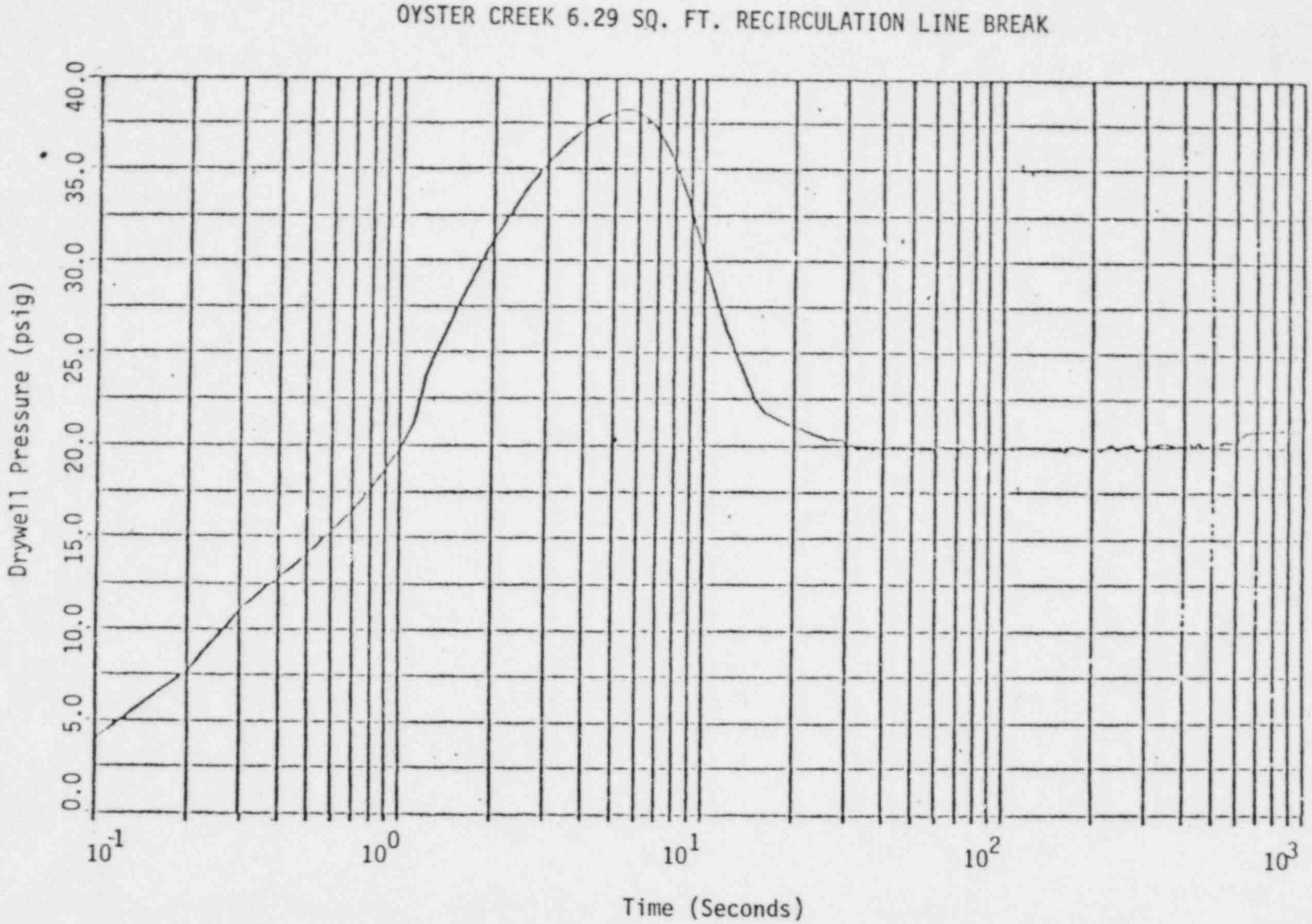

Figure 4. Drywell pressure response to a double-ended recirculation line break.

DRAFT

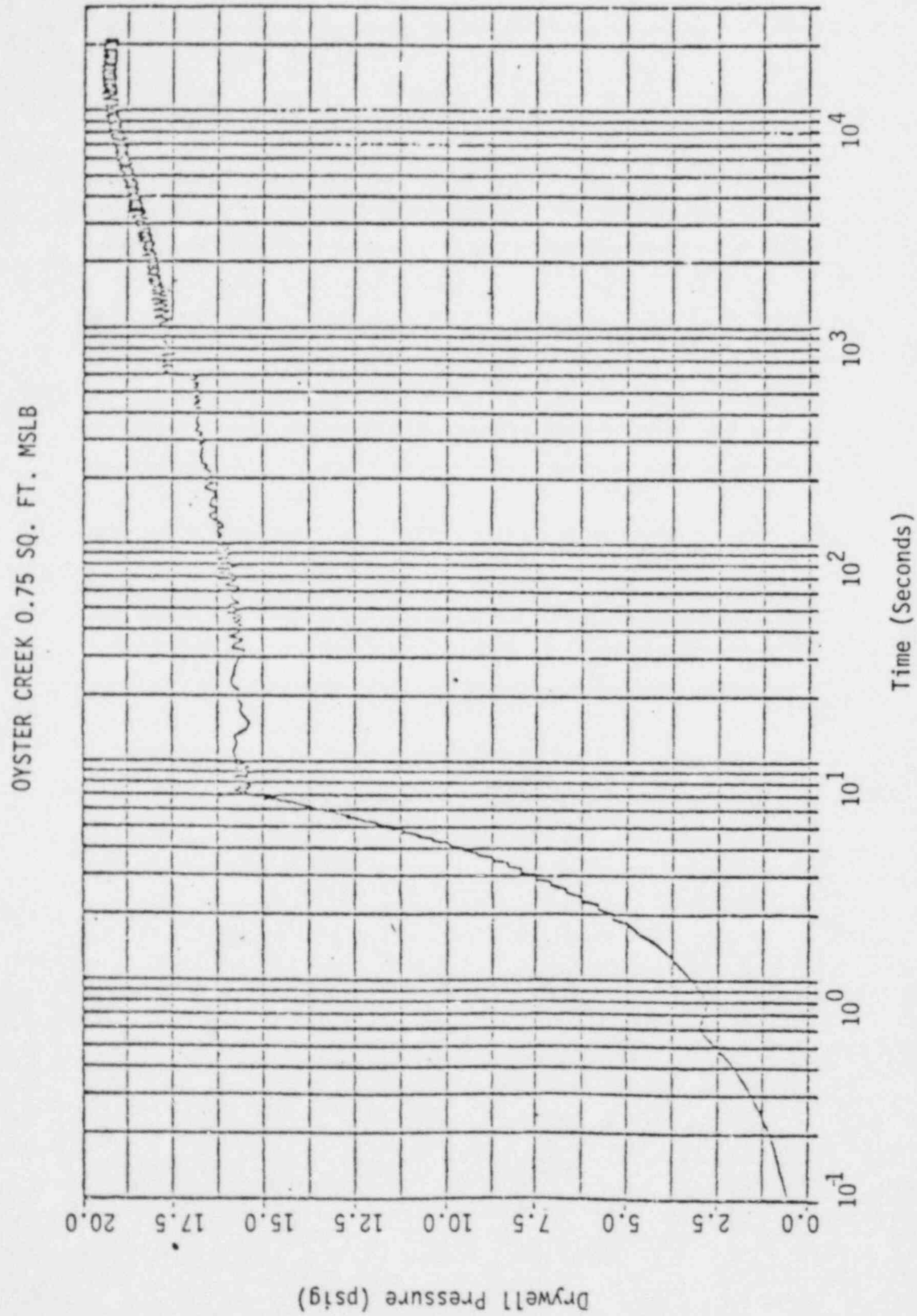

Figure 5. Drywell pressure response to a .75 ft^2 MSLB.

DRAFT

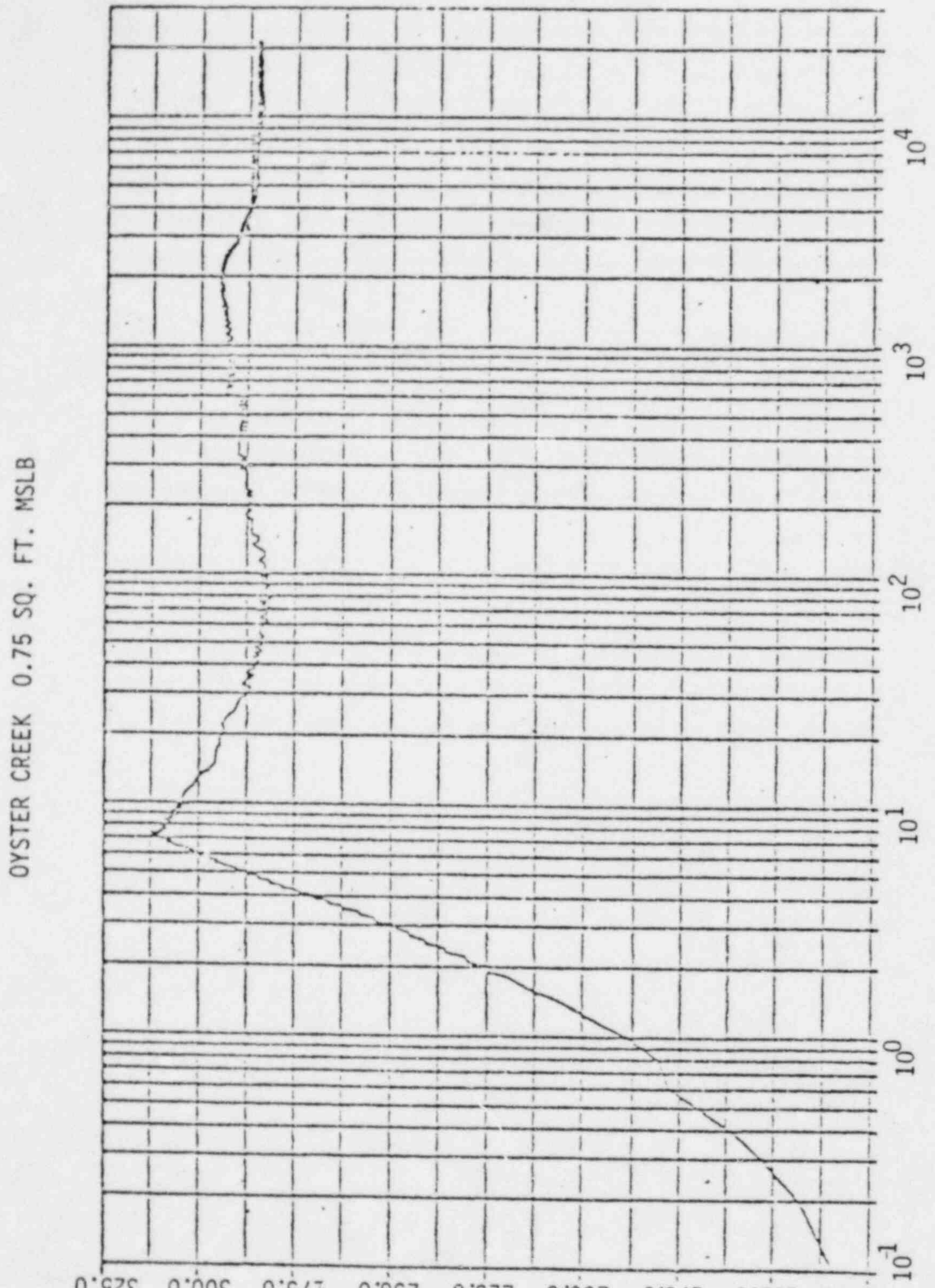

Figure 6. Drywell atmosphere temperature response to a .75 ft^2 MSLB.

DRAFT

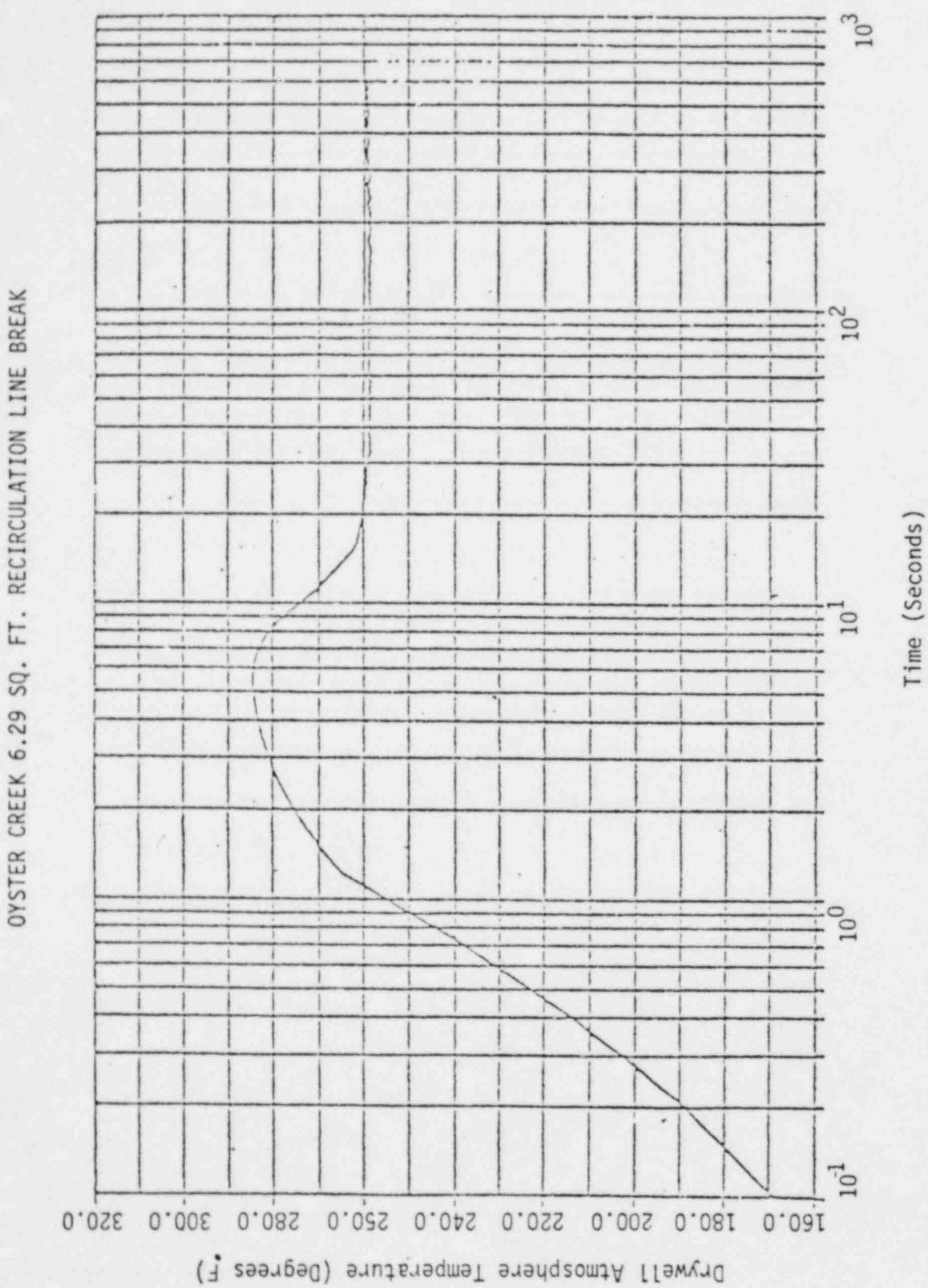

Figure 7. Drywell atmosphere temperature response to a double-ended recirculation line break.

DRAFT

The peak metal temperature caused by the 0.75ft^2 main steam line break was actually applied to the finite element model to calculate drywell thermal stresses. Table 1 shows the meridional and radial metal temperature values caused by the 0.75ft^2 main steam line break. The values shown in the table were extracted from results generated by the CONTEMPT-LT/02 computer code used in the post-accident mass and energy release analysis (Reference 1).

Table 1. Drywell metal temperatures.

ELEVATION (ft)	PLATE THICKNESS (in.)	INNER SURFACE TEMPERATURE (°F)	OUTER SURFACE TEMPERATURE (°F)
21.35	1.154	234	233
49.15	0.770	237	237
64.97	0.772	238	238
69.25	2.563	217	195
97.31	0.640	238	238
105.50	1.188	234	232

1.4 MATERIAL PROPERTIES

Reference 4 identifies the A 212 GR "B" plate and its equivalent ASME/ASTM designation as the material used in fabrication of the drywells. Young's Modulus and the coefficient of thermal expansion were extracted from Reference 3, Tables I-6.0 and I-5.0. Material property values used in this analysis are as follows:

MATERIAL	PROPERTY VALUE
A 212 GR "B" is equivalent to SA 515 GR "65" Plate	

DRAFT

MATERIAL	PROPERTY VALUE
(Young's Modulus)	30×10^6 psi
(Poisson ratio)	0.3
Minimum Yield Stress	35,000 psi
Coefficient thermal expansion	6.07×10^{-6} in/in/°F

1.5 PREVIOUS ANALYSES OF DRYWELL STRUCTURE

Many analyses have been performed for various lo. conditions. It is not our purpose to review all earlier work; therefore, only those analyses which deal with load combinations similar to those considered in this report will be reviewed.

Preliminary Description and Safety Analysis Report, Amendment 1, discusses the design-accident condition including deadweight, thermal, internal pressure, and earthquake loading. The drywell was designed for two loading scenarios: (1) internal pressure of 62 psig and 175°F metal temperature, and (2) 35 psig at metal temperature of 281°F. The maximum design pressure and temperature exceed the Design/Service conditions used in this report. A Housner spectrum with 0.22g peak ground acceleration was used in the analysis. It is not clear from the report how these loads were combined, but it is suspected that the peak stresses due to these loadings were not combined algebraically. It does not appear that a computer analysis was performed for any phase of the drywell stress analysis.

DRAFT

CHAPTER 2

ANALYSIS OF DRYWELL

2.1 ASSUMPTIONS

The drywell was analyzed using a finite element model for thermal, pressure, and deadweight loading conditions. The following assumptions were made in constructing the finite element model.

1. The structure and the loading were assumed to be axisymmetric; the penetrations and their effects were not considered.
2. The drywell was modeled assuming that the base of the shell was completely fixed to the foundation for translational and rotational movement.
3. The sand entrenchment was assumed to be linear elastic.
4. Thermal gradients were assumed to be linear.
5. The foam material between the drywell and the building was assumed to have no structural stiffness and was not included in the model.
6. A stress free temperature of 70°F was assumed.
7. The tongue and groove seal section at the top closure is considered a integral part of the structure; therefore, it was not modeled.
8. Pressure loading was calculated to be static, i.e., no dynamic effects of sudden pressurization were deemed necessary.

2.2 MATHEMATICAL MODEL

The finite element mathematical model of the drywell illustrated in Figure 8 was constructed based on the assumptions described in Section 2.1. A general purpose structural analysis program (ANSYS) which is outlined in Reference 5, was used to perform the stress computations. Axisymmetrical conical shell elements were used to model the structure. Sand entrenchment at the base of the drywell was modeled using spring elements.

DRAFT

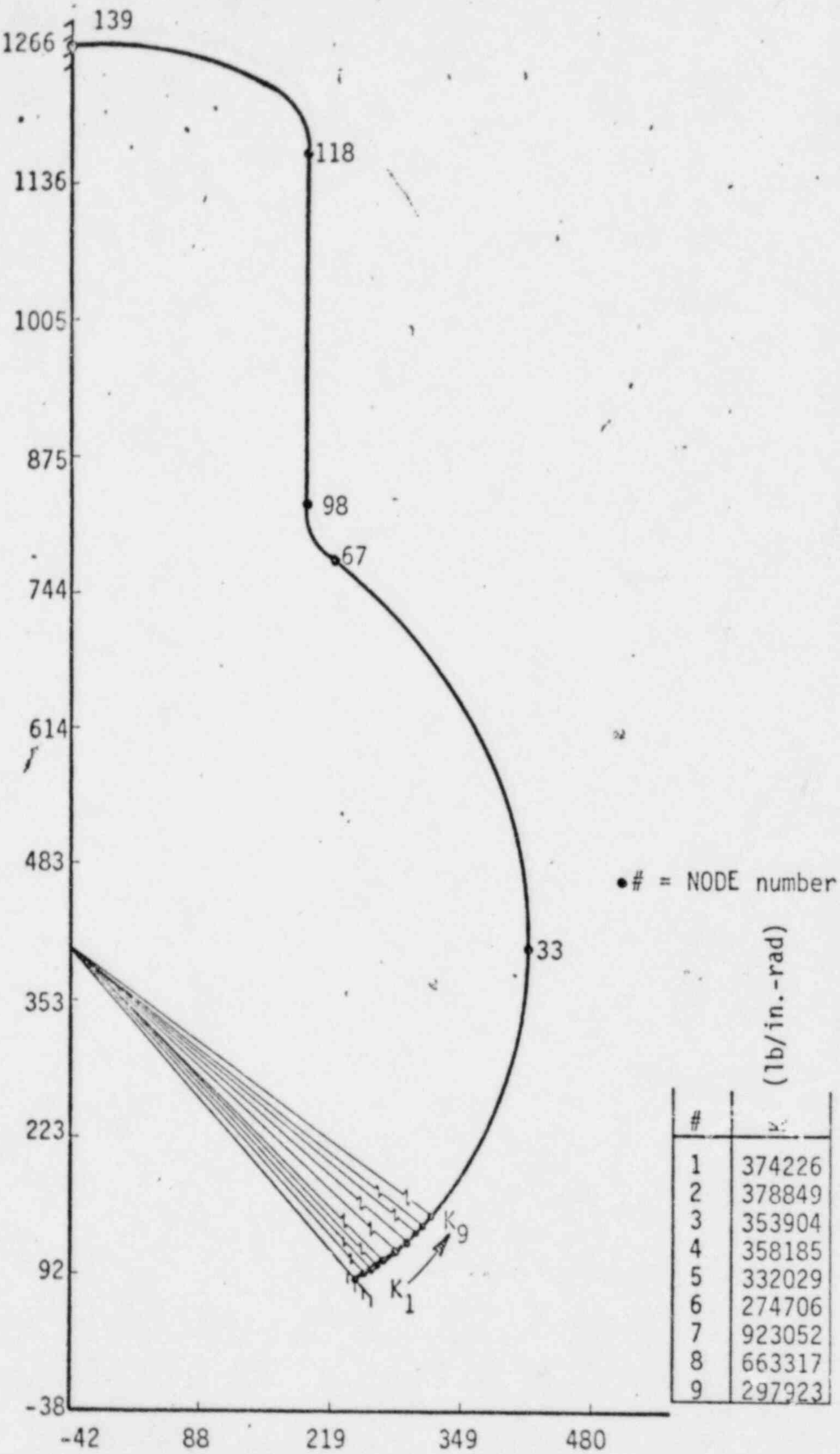

#	K (lb/in.-rad)
1	374226
2	378849
3	353904
4	358185
5	332029
6	274706
7	923052
8	663317
9	297923

Figure 8. Mathematical model of drywell structure.

DRAFT

The spring constraints that were used were based on data extracted from Reference 7, which used similar drywell geometry in all respects, except for a larger sphere radius. Constraints on the model included fixing the shell base at the 8.93 ft elevation for translation and rotational movement and fixing the top of the dome at the center line in the horizontal direction for symmetry. Verification of the model was performed by comparing deflection and stress results predicted by the finite element model against hand calculated values. In all cases the results compared were acceptable.

2.3 METHOD OF ANALYSIS

The above described finite element analysis presents directly meridional and circumferential membrane and bending stresses for the deadweight, pressure, and thermal loads.

The seismic loads were extracted from the results of the stick model analysis presented in Reference 2. The moment and shear due to SSE are depicted in Figures 2 and 3, respectively. These data were used to calculate the meridional membrane and shear stresses in this analysis. It was necessary to determine local bending stresses at the base of the structure due to seismic loading. This was accomplished by applying a pseudo-seismic horizontal load to the finite element model to produce the same fixed base global bending moment as that of the stick model.

Because a new site-specific spectrum with a peak ground acceleration of 0.17g's was approved, all seismic loadings were decreased by the ratio of 0.17/0.22 (Reference 8). Meridional membrane stresses were calculated by taking the bending moment values from Figure 2 and applying them to the appropriate drywell cross-section using the beam theory equation ($M/\pi R^2 t$). No hoop stresses were calculated for seismic loading. The shear stress was assumed to have a distribution of sin Ø along the circumferential direction, where Ø is measured from the positive direction

of seismic motion. Therefore, the maximum shear stresses in the drywell were calculated by taking the total shear loads presented in Figure 3 and dividing by πRt.

All membrane and bending stresses were combined by absolute sum for the appropriate code compliance criteria. The acceptance criterion used to establish structural adequacy for the drywell was Section III, of the ASME Boiler and Pressure Vessel Code - Subsection NE, July, 1977. Figure 9 illustrates locations on the drywell where the structure was considered to be in compliance with ASME definitions of Gross Structural Discontinuity and Local Primary Membrane stress regions. The remaining areas fall under General Membrane stress sections.

2.4 RESULTS OF ANALYSIS

Figures 10 through 12 illustrate the membrane and bending stresses generated by the finite element analysis for deadweight, pressure, and thermal loading, respectively. Figure 13 shows the stress results from the seismic analysis.

Verification of the finite element model was performed by comparing membrane stresses at the mid-section of the sphere and at the top of the dome against the closed form solution of $Pr/2t$ for pressure loading. Radial deflection due to thermal loading at the mid-section of the sphere was compared to the closed form solution of $R\alpha\Delta T$. In both cases the results compared were acceptable.

A study was performed to determine the effects of varying the spring stiffness used to model the sand entrenchment around the drywell at the base location. The thermal loading condition produced the highest stresses in this region; therefore, it was chosen as the loading condition to be studied. Three cases were analyzed using spring stiffnesses classified as strong, medium, and zero. The meridional bending stress was most

DRAFT

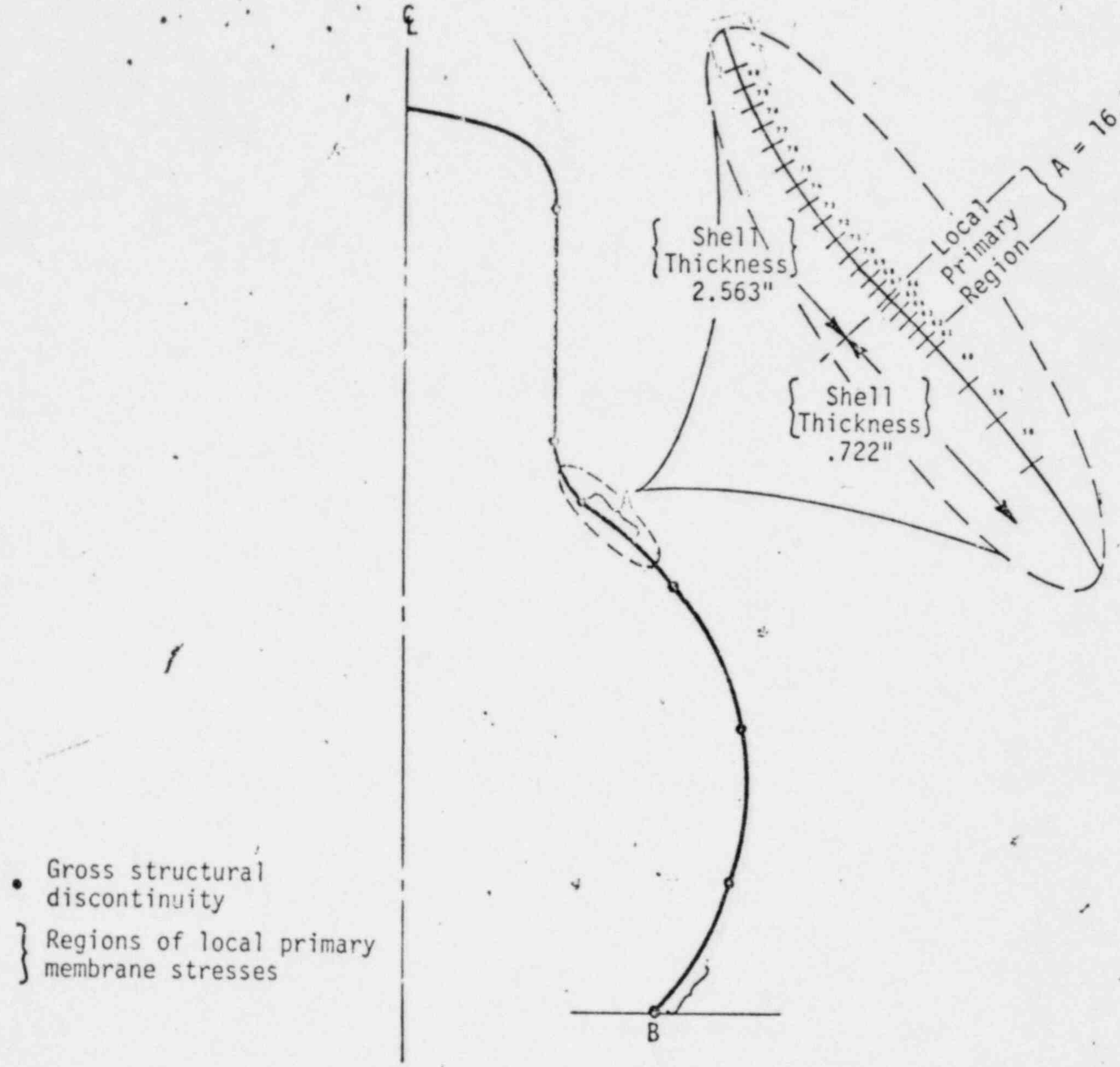

Figure 9. Drywell gross structural discontinuity and local primary membrane regions.

DRAFT

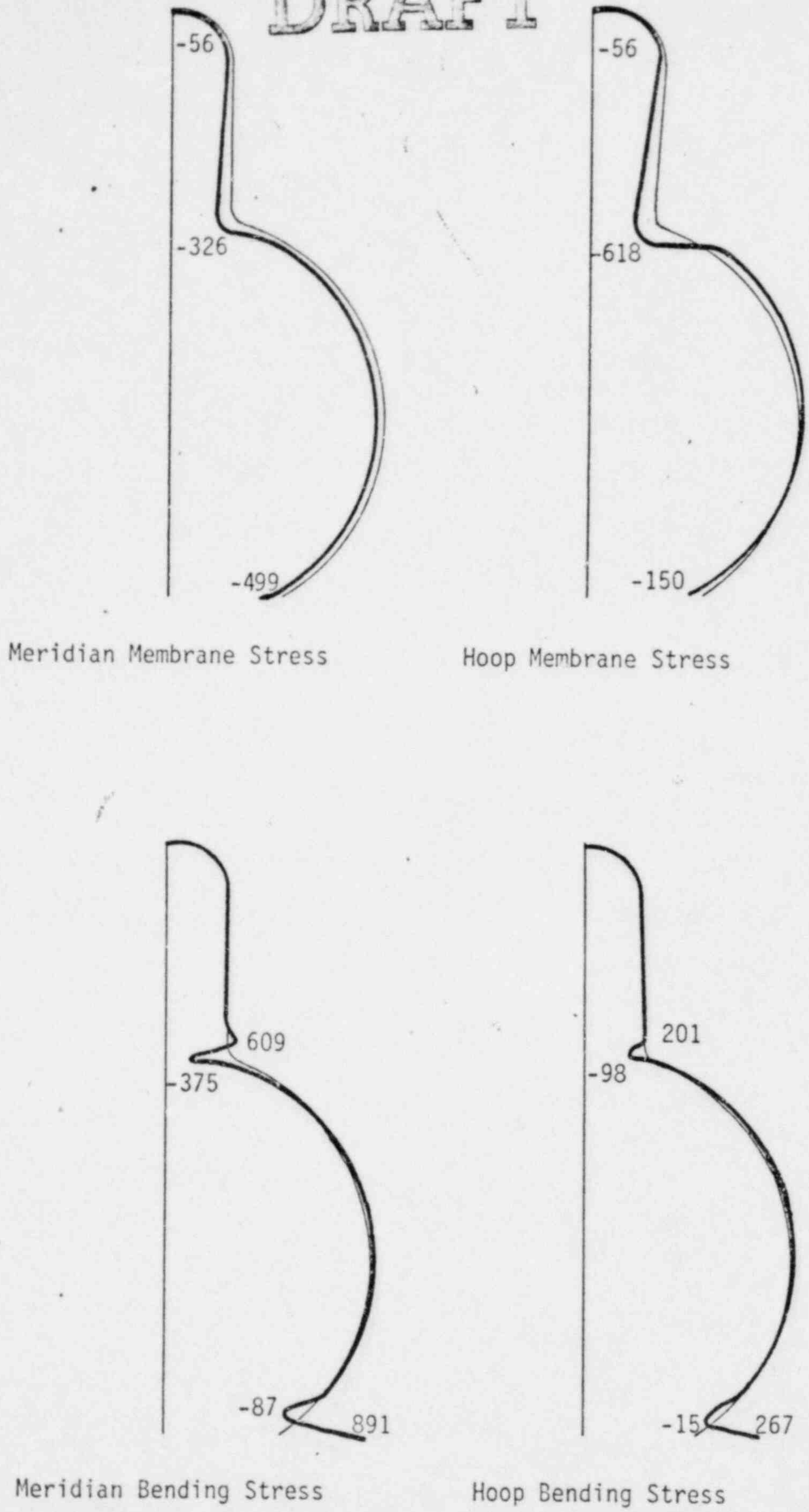

Figure 10. Dead load results (psi).

DRAFT

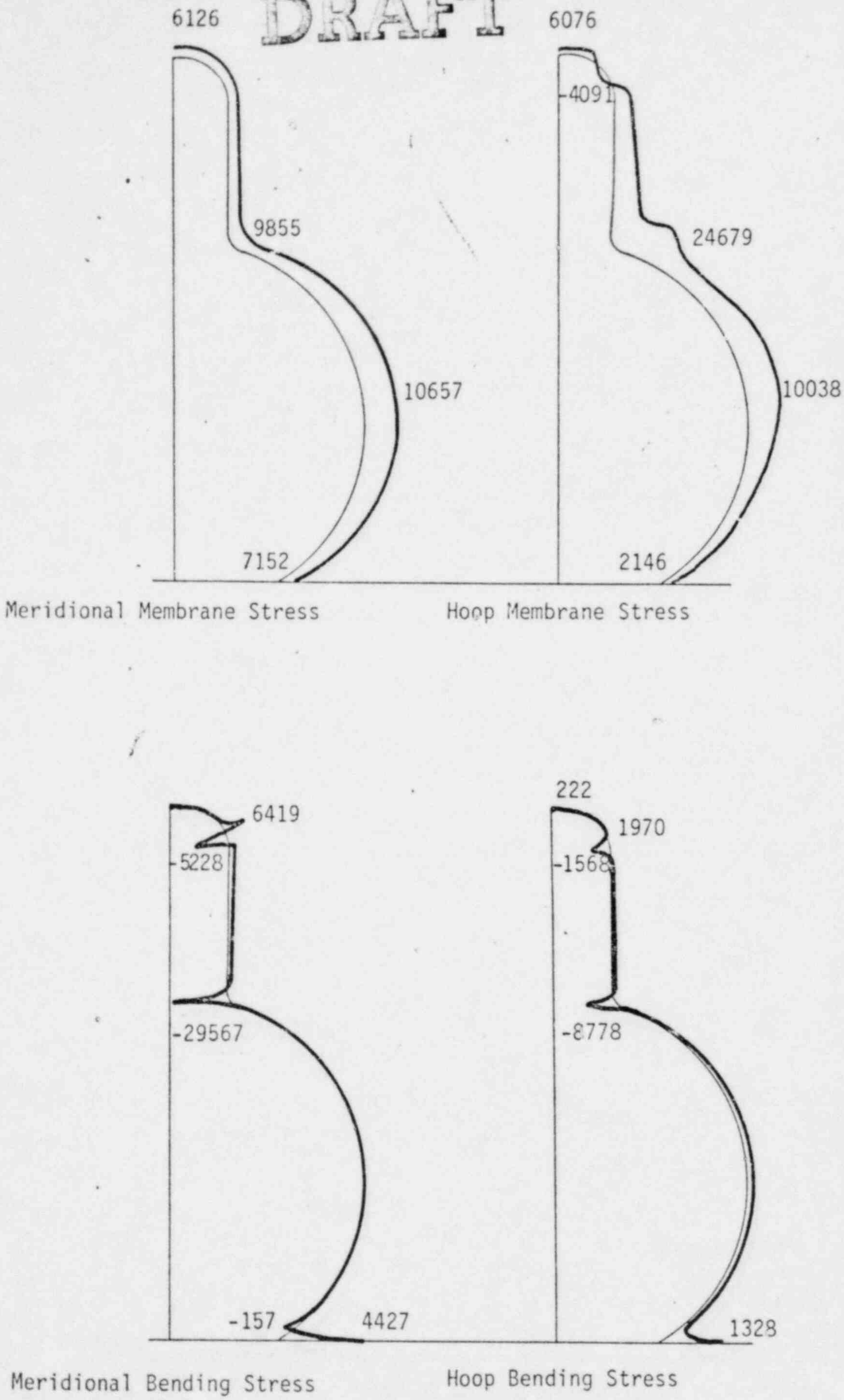

Figure 11. Pressure results (psi).

DRAFT

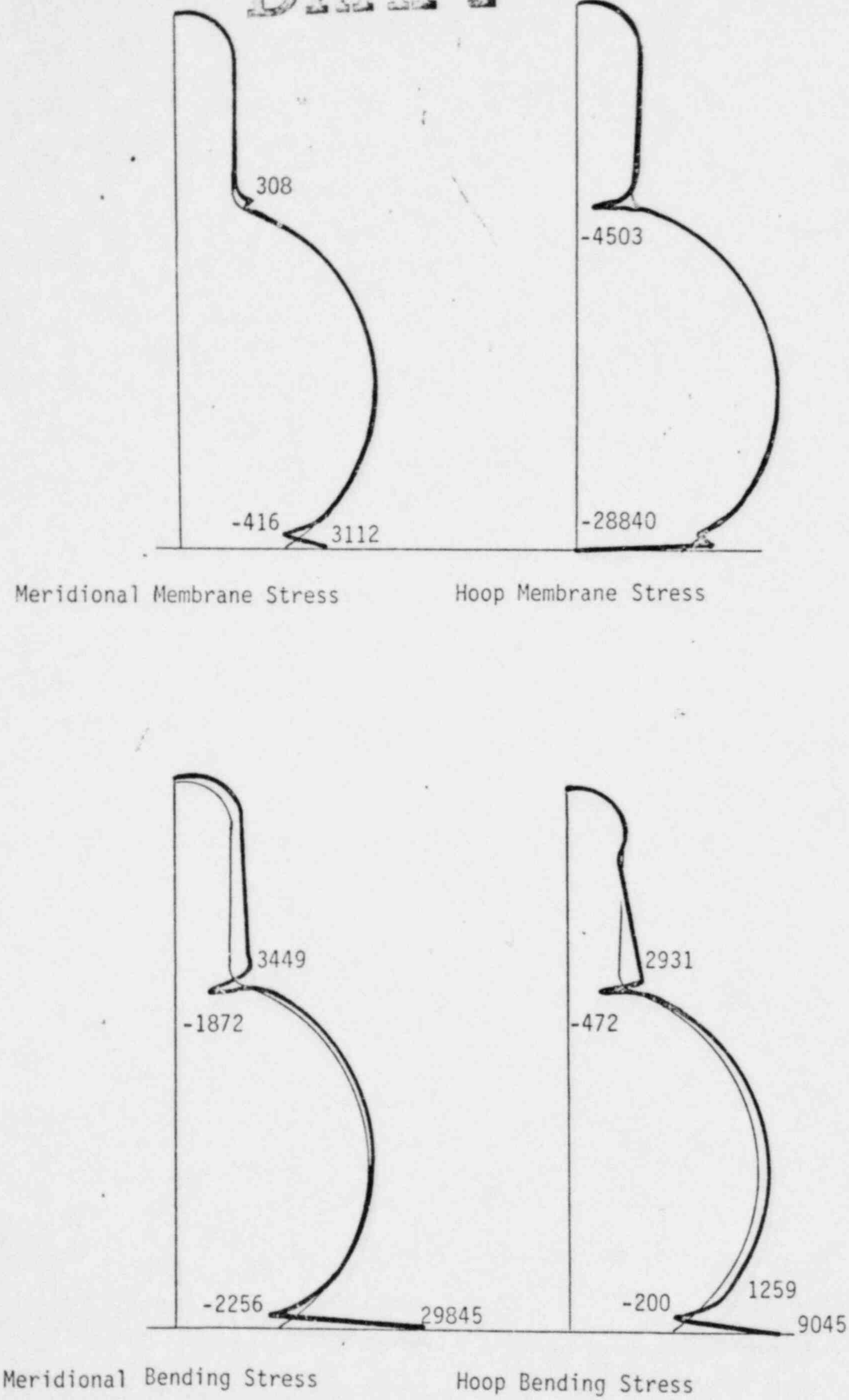

Figure 12. Thermal results (psi).

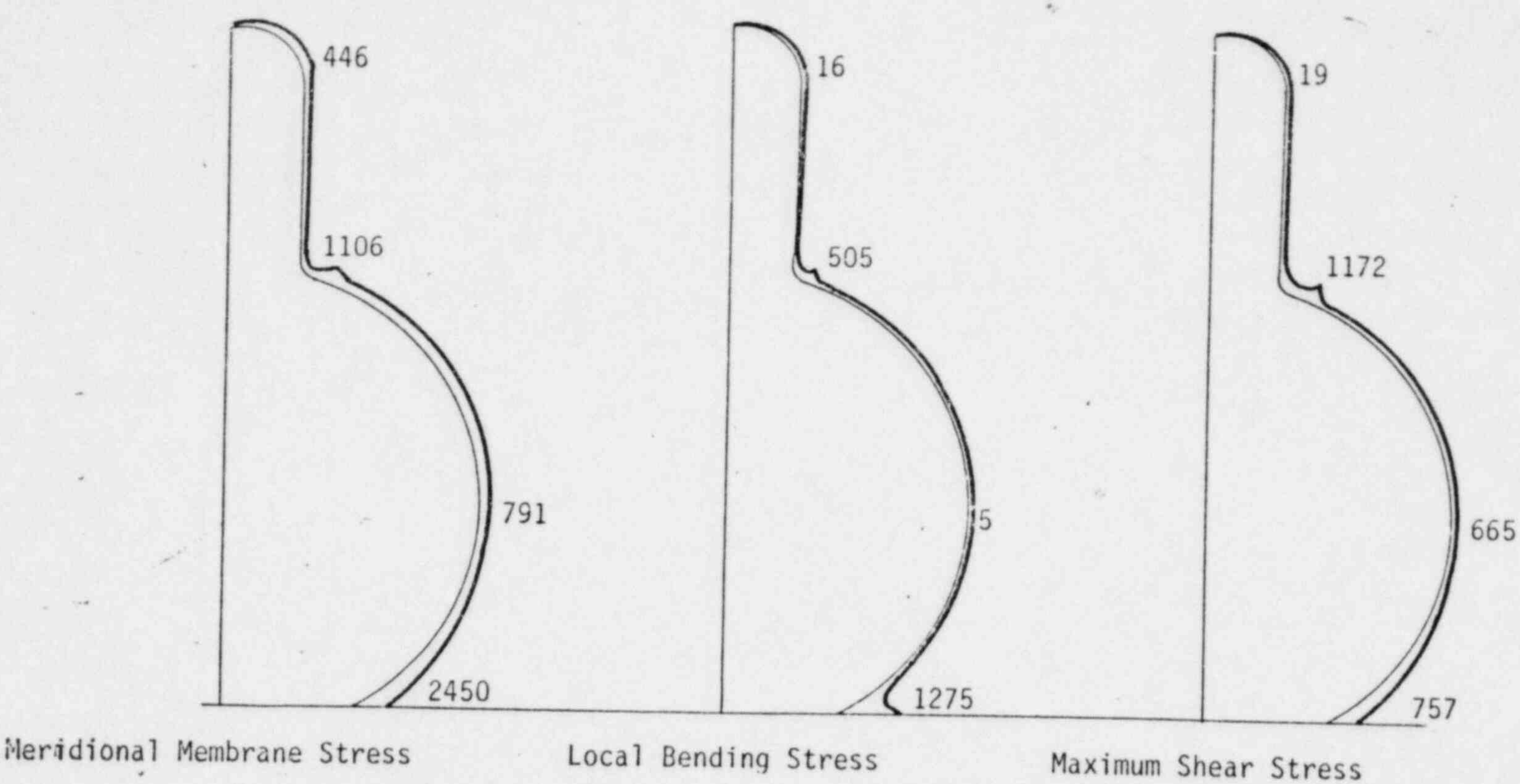

Figure 13. Seismic results (psi).

DRAFT

affected by the stiffness changes; the other membrane and bending stress results were relatively insensitive to stiffness change. The meridional bending stresses at the shell base were 51 ksi for zero stiffness, 30 ksi for medium stiffness, and 5 ksi for a strong spring stiffness.

It should be noted that even though the zero stiffness case would produce combined stress intensities that exceed the Service Condition requirements, there is relief in the Code under sub-paragraph NE 3228.3 that might allow the drywell design to be judged acceptable. In addition, the zero stiffness is actually a rather extreme condition. Any small stiffness in the sand will improve the bending stress a great deal. The stress results used to determine ASME code compliance are all based on a medium spring stiffness being used in the finite element model; this is virtually the same stiffness value as that presented in Reference 7.

Because the pressure loading rises sharply during a section of the transient (approximately 4.5 seconds), it was deemed prudent to verify that dynamic effects of this sudden pressurization could be neglected. A frequency analysis for Fourier Harmonic number = 0 was performed using the finite element model described in Section 2.1. The first mode frequency was determined to be approximately 22 Hz, which corresponds to a period of about 0.05 seconds. As a general rule, if the rise time of the loading (t_r) divided by the natural period of the structure (T) is greater than 4, the loading can be considered to be essentially static (Reference 9). In this case, the ratio t_r/T is approximately 90, assuming t_r = 4.5 sec. This implies that the pressure loading can be considered as static.

Meridional buckling compressive loads produced in the drywell at the lower portion of the sphere were caused by deadweight and seismic loading. These compressive loads are not axisymmetric because seismic loads produce compression on one side and tension on the opposite side. It is difficult, therefore, to determine critical stresses because most published buckling analyses pertain to axisymmetric loading on simple geometric structures.

DRAFT

The method used to determine the critical load for meridional buckling of the drywell consisted of employing two different axisymmetric buckling analyses: externally pressurized sphere analysis and axially loaded truncated shell analysis. Both of these analyses were similar in geometry to that of the drywell. In both cases, the critical meridian buckling stresses exceeded the drywell stress by a factor of five. If thermal or pressure loads, were superimposed on these compressive loads they would put the shell in tension and therefore eliminate the need to check for meridional buckling loads. This is not the case for the predicted circumferencial critical buckling stress at the base, which is estimated at -15.00 ksi versus - 28.5 ksi for the thermal stresses. The critical buckling stress was calculated assuming that the sphere had a uniform external pressure applied to its outer surface. This loading condition would produce a uniform membrane stress in the sphere, which is not what would take place in the drywell sphere because the compressive circumferential stress is confined to a narrow ring at the base location. For this reason the calculated critical circumferential buckling stress is judged to be extremely conservative; however, for lack of a better solution it was used for comparison. It is possible that some amount of circumferencial buckling could occur at the base location due to thermal loading. It should be noted that no credit was taken for the structural effect of the concrete that extends upward from the foundation around the inside of the drywell. This concrete will surely help structural stability in this lower region, and greatly reduce the chance of circumferential buckling.

After combining maximum stresses produced at various locations of the drywell, it was determined that the critical location for Design Conditions was where the sphere curves inwards to the cylindrical section (Region A on Figure 9). The critical location for Service Conditions is at the base of the drywell. Table 2 includes maximum general membrane stresses; Tables 3 and 4 present the stress values used for ASME Code Design condition compliance for local primary membrane regions. Table 5 is for Service Level compliance.

DRAFT

Table 2. P_m Values Summary, Design Condition

Loading Condition	Element Number	σφ (psi)	σθ (psi)	T (psi)
Deadweight	67	-72	-545	0
Pressure	67	2275	22275	0
Seismic	67	±324	0	±340
Sum Σ		2527	21730	340

$$P_m = \frac{\sigma\phi + \sigma\theta}{2} \pm \sqrt{\left(\frac{\sigma\phi - \sigma\theta}{2}\right)^2 + T^2} = 21736 \text{ psi} > S_m = 17{,}800 \text{ psi}$$

Table 3. P_L Values, Design Condition

Loading Condition	Element Number	σφ (psi)	σθ (psi)	T (psi)
Deadweight	66	-317	-618	0
Pressure	66	9855	24679	0
Seismic	66	±1106	0	±1112
Sum Σ		10646	24069	1112

$$P_L = \frac{\sigma\phi + \sigma\theta}{2} \pm \sqrt{\left(\frac{\sigma\phi - \sigma\theta}{2}\right)^2 + T^2} = 24161 \text{ psi} \leq 1.5\ S_m = 26{,}700 \text{ psi}$$

Table 4. (P_m or P_L) + P_b Values, Design Condition

DRAFT

Loading Condition	Element Number	Membrane Stress		Bending Stress		
		$\sigma\phi$	$\sigma\theta$	$\sigma\phi$	$\sigma\theta$	T
Deadweight	63	-326	-317	0	27	0
Pressure	63	10356	20362	-1317	-152	0
Seismic	63	±1075	0	407	0	±1142
Sum Σ		11105	20045	-1724	-752	1142

$(\sigma\phi)_{Total} = 11105 + |-1724| = 12829$

$(\sigma\theta)_{Total} = 20045 + |-725| = 20770$

T = 1142 psi

$$S.I. = \frac{(\sigma\phi)_{Total} + (\sigma\theta)_{Total}}{2} \pm \sqrt{\left(\frac{(\sigma\phi)_{Total} + (\sigma\theta)_{Total}}{2}\right)^2 + T^2}$$

$= 20931 \text{ psi} \leq 1.5\ S_m = 26{,}700 \text{ psi}$

Table 5. Total stress at base location, Service Condition.

Loading Description	Membrane Stress		Bending Stress		
	$\sigma\phi$	$\sigma\theta$	$\sigma\phi$	$\sigma\theta$	T
Deadweight	-499	-150	891	267	0
Pressure	7152	2146	4427	1328	0
Seismic	±2450	0	±1275	0	±757
Thermal	3112	-28840	29845	9045	0
Sum Σ	12215	-26844	36438	10640	757

$(\sigma\phi)_{Total} = 12215 + 36438 = 48653 \text{ psi}$

$(\sigma\theta)_{Total} = |-26844| + 10640 = 37484 \text{ psi}$

T = 757 psi

$$S.I. = \frac{(\sigma\phi)_{Total} + (\sigma\theta)_{Total}}{2} \pm \sqrt{\left(\frac{(\sigma\phi)_{Total} - (\sigma\theta)_{Total}}{2}\right)^2 + T^2}$$

$= 48704 \text{ psi} \leq 3S_m = 53400 \text{ psi}$

Deadweight, pressure, and seismic loading apply for "Design Conditions Only"; thermal loading is not considered. The following conditions must be satisfied for code compliance:

$P_m \leq S_m$

$P_L \leq 1.5\ S_m$

$(P_L \text{ or } P_m) + P_b \leq 1.5\ S_m$

Deadweight, pressure, seismic, and thermal loading apply for Service Conditions. The following conditions must be satisfied for code compliance:

$(P_m \text{ or } P_L) + P_b + Q \leq 3\ S_m$

P_m is the general primary membrane stress. P_L is the local primary membrane stress. P_b is the bending stress. Q is the secondary stress. The definitions for P_m, P_L, P_b and Q are described in the ASME code. In this study, Q is the bending stress at gross structural discontinuities. The values of S_m can be found in Table I-10.0, Appendix A of the ASME code.

The sum of general membrane stresses (P_m) listed in Table 2 do not meet the general primary membrane stress intensity requirements of $P_m \leq$ 1.0 Sm. The region where the general primary membrane stresses exceed the allowable is immediately adjacent to the local primary region (Region A of Figure 9). Even the most lenient interpretation of the local primary region would require that the local primary region be extended approximately 11 in. upwards before the general membrane stress profile in this region would drop below the 1.0 S_m value. The local membrane stress intensity, primary membrane stress intensity, and primary plus secondary stress intensity shown in Tables 3, 4, and 5 respectively all meet the stress intensity limits specified by the ASME Code. It should be noted that the

DRAFT

large meridional and hoop bending stresses illustrated in Figure 11 are classified as secondary stresses because they are caused by a gross structural discontinuity, but these bending stresses combined with the membrane stresses will produce a stress intensity of 39.4 ksi that exceeds the minimum yield stress of the material.

DRAFT

CHAPTER 3
SUMMARY AND CONCLUSION

The drywell containment structure was analyzed for four combined load conditions: deadweight, accident pressure (P_{max} = 37 psig), thermal loads (Tmax = 238°F), and seismic loads from a 0.17g peak ground acceleration, Reg. Guide 1.60 spectra. The maximum stress intensity produced in the drywell was 48.7 ksi at the base location. All stresses in the drywell were within the stress intensity limits of the Design and Service Conditions given by the ASME-Boiler and Pressure Vessel Code, Section III, 1977, subsection NE, except for the general membrane stress adjacent to Region A on Figure 9. It is difficult to predict how the stresses in this region of the drywell would redistribute themselves if yielding were to occur due to the 39.4 ksi stress intensity at the thin side of the structural discontinuity where the .722 in. and 2.563 in. plates meet. The high stress intensities in this region are generated by mechanical loads which are different in nature to the thermal stresses that produce the maximum stress intensity at the location. It should be noted that a limit or plastic analysis in this region may show that ASME compliance could be met; however, this has not been verified.

The meridional critical buckling stress is estimated to be five times the meridional compressive stress calculated for deadweight and seismic loading. The calculated circumferential critical buckling stress is less than the 28.8 ksi circumferential compressive stress produced at the base due to thermal loading. There could be some localized circumferential buckling at the base of the structure, but the self-limiting nature of thermal stresses suggest that no adverse structural degradation will appear. It should be noted that no credit was taken for the structural effect of the concrete that extends upward from the drywell base. This would certainly lower any chance that buckling would occur.

DRAFT

REFERENCES

1. D. G. Vreeland, "Mass and Energy Release for Possible Pipe Break Inside Containment, Containment Pressure and Heat Removal Capability for Oyster Creek Nuclear Power Plant," Lawrence Livermore National Laboratory, Livermore, California, letter report addressed to I. R. Finfrock, Jr.

2. R. C. Murray, T. A. Nelson, S. M. Ma, J. D. Stevenson, "Seismic Review of the Oyster Creek Nuclear Power Plant as Part of the Systematic Evaluation Program," Nureg/Cr-1981.

3. ASME Boiler and Pressure Vessel Code, Section III, 1977 Edition, Appendices.

4. S. W. Chous, Burns and Roe Inc., letter addressed to Y. Nogai, Oyster Creek Nuclear Station SPE Seismic Evaluation Program.

5. ANSYS Engineering Analysis System User's Manual, Swanson Analysis System Inc., Houston, Pennsylvania.

6. Jersey Central Power and Light Company, Facility Description and Safety Analysis Report, Volume 1, NRC Docket Item 50219-1.

7. "Seismic Safety Margin Evaluation Reactor Building Primary Coolant Loop, Big Rock Point Nuclear Power Plant," D'Appolonia for Consumer Power.

8. "Site Specific Ground Response Spectra for SEP Plants Located in the Eastern United States," Letter to all SEP Owners from Dennis Crutchfied, NRC.

9. Biggs, J. M., Introduction to Structural Dynamics, McGraw-Hill Book Company, New York, New York, 1964.